J Stat Phys
DOI 10.1007/s10955-009-9914-y

Switching Phenomena in a System with No Switches

Tobias Preis · H. Eugene Stanley

Received: 8 November 2009 / Accepted: 23 December 2009

Abstract It is widely believed that switching phenomena require switches, but this is actually not true. For an intriguing variety of switching phenomena in nature, the underlying complex system abruptly changes from one state to another in a highly discontinuous fashion. For example, financial market fluctuations are characterized by many abrupt switchings creating increasing trends ("bubble formation") and decreasing trends ("financial collapse"). Such switching occurs on time scales ranging from macroscopic bubbles persisting for hundreds of days to microscopic bubbles persisting only for a few seconds. We analyze a database containing 13,991,275 German DAX Future transactions recorded with a time resolution of 10 msec. For comparison, a database providing 2,592,531 of all S&P500 daily closing prices is used. We ask whether these ubiquitous switching phenomena have quantifiable features independent of the time horizon studied. We find striking scale-free behavior of the volatility after each switching occurs. We interpret our findings as being consistent with time-dependent collective behavior of financial market participants. We test the possible universality of our result by performing a parallel analysis of fluctuations in transaction volume and time intervals between trades. We show that these financial market switching processes have properties similar to those of phase transitions. We suggest that the well-known catastrophic bubbles that occur on large time scales—such as the most recent financial crisis—are no outliers but single dramatic representatives caused by the switching

Supplementary information can be found on http://www.tobiaspreis.de.

T. Preis · H.E. Stanley (✉)
Center for Polymer Studies, Department of Physics, 590 Commonwealth Avenue, Boston, MA 02215, USA
e-mail: hes@bu.edu

T. Preis
e-mail: mail@tobiaspreis.de

T. Preis
Institute of Physics, Johannes Gutenberg University Mainz, Staudinger Weg 7, 55128 Mainz, Germany

T. Preis
Artemis Capital Asset Management GmbH, Gartenstr. 14, 65558 Holzheim, Germany

Published online: 05 January 2010

between upward and downward trends on time scales varying over nine orders of magnitude from very large ($\approx 10^2$ days) down to very small (≈ 10 ms).

Keywords Econophysics

1 Introduction

In physics and in other natural sciences, it is often a successful strategy to analyze the behavior of a system by studying the smallest components of that system. For example, the molecule is composed of atoms, the atom consists of a nucleus and electrons, the nucleus consists of protons and neutrons, and so on. The fascinating point about analyses on steadily decreasing time and length scales is that one often finds that the system exhibits properties which cannot only be explained by the properties of its components alone. Instead, a complex behavior can emerge due to the interactions among these components [1]. In financial markets, these components are comprised by the market participants who buy and sell assets in order to realize their trading and investment decisions. The superimposed flow of all individual orders submitted to the exchange trading system initiated by market participants generate a complex system with fascinating properties, similar to physical systems.

One of the key conceptual elements in modern statistical physics is the concept of scale invariance, codified in the scaling hypothesis that functions obey certain functional equations whose solutions are power laws [2, 3]. The scaling hypothesis has two categories of predictions, both of which have been remarkably well verified by a wealth of experimental data on diverse systems. The first category is a set of relations, called *scaling laws*, that serve to relate the various critical-point exponents characterizing the singular behavior of functions such as thermodynamic functions. The second category is a sort of *data collapse*, where under appropriate axis normalization, diverse data "collapse" onto a single curve called a scaling function.

Econophysics research has been addressing a key question of broad interest for both scientific and practical reasons: quantifying and understanding *large* stock market fluctuations. Previous work focussed on the challenge of quantifying the behavior of the probability distributions of large fluctuations of relevant variables such as returns, volumes, and the number of transactions. Sampling the far tails of such distributions requires a large amount of data. There is a truly gargantuan amount of pre-existing precise financial market data already collected, many orders of magnitude more than for typical complex systems. Accordingly, financial markets are becoming a paradigm of complex systems, and increasing numbers of scientists are analyzing market data [4–17]. Empirical analyses have been focused on quantifying and testing the robustness of power-law distributions that characterize large movements in stock market activity. Using estimators that are designed for serially and cross-sectionally independent data, findings support the hypothesis that the power law exponents that characterize fluctuations in stock price, trading volume, and the number of trades [18–25] are seemingly "universal" in the sense that they do not change their values significantly for different markets, different time periods, or different market conditions.

In contrast to these analyses of global financial market distributions, we focus on the temporal sequence of fluctuations in volatility, transaction volume, and inter-trade times before and after a trend switching point. Our analysis can provide insight into switching processes in complex systems in general and financial systems in particular. The study of dramatic crash events is limited by the fortunately rare number of such events. Increasingly, one seeks to understand the current financial crisis by comparisons with the depression of

the 1930's. Here we ask if the smaller financial crises—trend switching processes on all time scales—also provide information of relevance for large crises. If this is so, then the large abundance of data on smaller crises should provide quantifiable statistical laws for the concept which we call "*bubbles on all scales*."

2 Financial Market Data

To answer whether smaller financial crises also provide information of relevance to large crises, we perform parallel analyses of bubble formation and bursting using two different data sets on two quite different time scales: (i) from $\approx 10^1$ ms to $\approx 10^6$ ms, and (ii) from $\approx 10^8$ ms to $\approx 10^{10}$ ms.

2.1 German Market—DAX Future

For the first analysis, we use a multivariate time series of the German DAX Future contract (FDAX) traded at the European Exchange (Eurex), which is one of the world's largest derivatives exchanges. A "futures" exchange or derivatives exchange is a central financial exchange where people can trade standardized "futures contracts". A "future" is a contract to buy or sell an underlying asset at a specified price at a specific future date—in this case the German DAX index, which measures the performance of the 30 largest German companies in terms of order book volume and market capitalization.[1] The time series comprises $T_1 = 13{,}991{,}275$ transactions of three disjoint three-month periods (see Table 1). Each end of the three disjoint periods corresponds to a last trading day of the FDAX contract, which is ruled to be the third Friday of one of the months March, June, September, and December, apart from the exceptions of national holidays. The data set we analyze contains the transaction prices, the volumes, and the corresponding time stamps [30–33], with a large liquidity and inter-trade times down to 10 ms, which allows us to perform an analysis of microtrends.

The time series analysis of future contracts has the advantage that the prices are created by trading decisions alone. In contrast, stock index data are derived from a weighted sum of a bunch of stock prices. Furthermore, systematic drifts by inflation are eliminated by construction. The theory of futures pricing based on arbitrage states that for an asset that can be stored at no cost and which does not yield any cash flows, the futures price F has to be equal to the spot price S plus the cost of financing the purchase of the underlying between

Table 1 Three disjoint three-month periods of the German DAX Future contract (FDAX) which we analyze. Additionally, the mean volume per transaction $\bar{v}$ and the mean inter-trade time $\bar{\tau}$ are shown

Contract	Records	Time Period	$\bar{v}$	$\bar{\tau}$ [s]
FDAX JUN 2007	3,205,353	16 March 2007–15 June 2007	3.628[a]	2.485[b]
FDAX SEP 2008	4,357,876	20 June 2008–19 September 2008	2.558[a]	1.828[b]
FDAX DEC 2008	6,428,046	19 September 2008–19 December 2008	2.011[a]	1.253[b]

[a]measured in units of contract

[b]including overnight gaps

[1]More detailed informations about German DAX index constituents and calculation principles can be found on http://www.deutsche-boerse.com.

the spot date and the expiry date [34, 35]. This theoretical futures price can be referred to as *fair value*. In the case of the German DAX index, the underlying purchase can be financed till expiry with a loan rate. Using a continuously compounded rate r, the *fair value* equation can be written as

$$F(t) = S(t)e^{rt}, \tag{1}$$

whereas t denotes the remaining time till expiry. The theoretical futures price expression—see (1)—which simply reflects the *cost of carry*, compensates interest rate related effects. At expiry time $t = 0$, the future's price and underlying price are identical.

2.2 US Market—S&P500 Stocks

For the second analysis, which focuses on macrotrends, we use price time series of daily closing prices of all stocks of the S&P500 index. This index consists of 500 large-cap common stocks, which are actively traded in the United States of America.[2] The time series comprises $T_2 = 2{,}592{,}531$ closing prices overall of all US stocks which were constituent of the S&P500 on June 16, 2009. Our oldest closing prices date back to January 2, 1962. The data base of closing prices we analyzed contains the daily closing prices and the daily cumulative trading volume. As spot market prices undergo a significant shift by inflation over time periods of more than 40 years, we study the logarithm of stock prices instead of the raw closing prices. Thus, the results between the two different data bases on two quite different time scales become more comparable.

3 Renormalization Method

Less studied than the large fluctuations of major national stock indices such as the S&P500 are the various jagged functions of time characterizing complex financial fluctuations down to time scales as short as a few milliseconds. These functions are not amenable to mathematical analysis, at first sight because they are characterized by sudden reversals between up and down microtrends (see Fig. 1), which can also be referred to as microscopic *bubbles* on small time scales. On these small time scales, evidence can be found [9] that the three major financial market quantities of interest—price, volume, and inter-trade times—are connected in a complex way, overburdening standard tools of time series analysis such as linear cross-correlation analysis. Thus, more sophisticated methods are necessary to analyze these complex financial fluctuations creating complex financial market patterns.

It is not trivial how to characterize the sudden microtrend reversals, as the time derivative of the price $p(t)$ is discontinuous. This behavior is completely different from most real world trajectories, e.g. a football, for which the time derivative of the space-time-relationship is a smooth continuous function. In the following, we find a way of quantitatively analyzing these sudden microtrend reversals which exhibit a behavior analogous to phase transitions [36], and we interpret these transitions in terms of the cooperative interactions of the traders involved. A wide range of examples of transitions exhibiting scale-free behavior ranges from magnetism in statistical physics to heartbeat intervals (sudden switching from heart contraction to heart expansion) [37], and to macroscopic social phenomena such as traffic flows (switching from a free to congested traffic) [38].

[2] More detailed informations about S&P500 constituents and calculation principles can be found on http://www.standardandpoors.com.

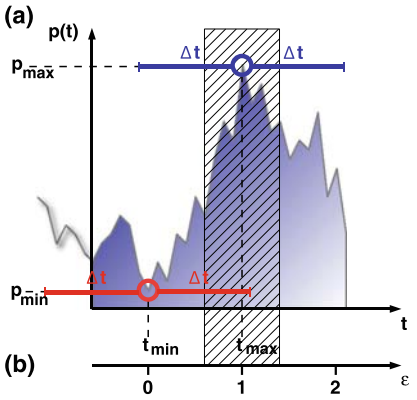

Fig. 1 Visualization of a *microtrend* in the price movement $p(t)$. (**a**) Positive microtrend of order Δt starting at a local price minimum $p_{\min}$ and ending at a local price maximum $p_{\max}$. The *hatched region* around $p_{\max}$ indicates the interval in which we find scale-free behavior of related quantities—volume and inter-trade time. This behavior is consistent with "self-organized" [26] macroscopic interactions among many traders [27], not unlike "tension" in a pedestrian crowd [28, 29]. The reason for tension among financial traders may be found in risk aversions and profit targets of financial market participants. (**b**) Renormalized time scale ε between successive extrema, where $\varepsilon = 0$ corresponds to the start of a microtrend, and $\varepsilon = 1$ corresponds to the end

To focus on switching processes of price movements down to a microscopic time scale, we first propose how a switching process can be quantitatively analyzed. Let $p(t)$ be the transaction price of trade t, which will be treated as a discrete variable $t = 1, \ldots, T$. Each transaction price $p(t)$ is defined to be a *local maximum* $p_{\max}(\Delta t)$ of order Δt, if there is no higher transaction price in the interval $t - \Delta t \leq t \leq t + \Delta t$. Thus, if $p(t) = p_{\max}(t, \Delta t)$, $p(t)$ is a *local maximum*, where

$$p_{\max}(t, \Delta t) = \max\{p(t) | t - \Delta t \leq t \leq t + \Delta t\}. \tag{2}$$

Analogously, each transaction price $p(t)$ is defined to be a *local minimum* of order Δt, if there is no lower transaction price in this interval. With

$$p_{\min}(t, \Delta t) = \min\{p(t) | t - \Delta t \leq t \leq t + \Delta t\}, \tag{3}$$

it follows that $p(t)$ is a *local minimum* if $p(t) = p_{\min}(t, \Delta t)$. In this sense, the two points in the time series in Fig. 1 marked by circles are a local minimum and a local maximum, respectively.

For the analysis of financial market quantities in dependence of trend fraction, we introduce a renormalized time scale ε between successive extrema as follows: Let $t_{\min}$ and $t_{\max}$ be the time (measured in units of ticks) at which the corresponding transactions take place of a successive pair of *local minimum* and *local maximum* (see Fig. 1). For a positive microtrend, the renormalized time scale is given by

$$\varepsilon(t) \equiv \frac{t - t_{\min}}{t_{\max} - t_{\min}}, \tag{4}$$

with $t \geq t_{\min}$, and for a negative microtrend by

$$\varepsilon(t) \equiv \frac{t - t_{\max}}{t_{\min} - t_{\max}}, \tag{5}$$

with $t \geq t_{\max}$. Thus, $\varepsilon = 0$ corresponds to the beginning of the microtrend and $\varepsilon = 1$ indicates the end of the microtrend. We analyze a range of ε within the interval $0 \leq \varepsilon \leq 2$, so we can analyze trend switching processes both before and after the critical value $\varepsilon = 1$ (Fig. 1). The renormalization is essential to assure that microtrends of various lengths can be aggregated and that all switching points have a common position on the renormalized time scale.

3.1 Volatility Analysis

First we analyze the fluctuations $\sigma^2(t)$ of the price time series during the short time interval of increasing microtrends from one price minimum to the next price maximum (see Fig. 2a) and decreasing microtrends from one price maximum to the next price minimum (see Fig. 2b). The quantity studied is given by squared price differences, $\sigma^2(t) = (p(t) - p(t-1))^2$ for $t > 1$, and can be referred to as local volatility. For the analysis of $\sigma^2(t)$ in dependence of the trend fraction, we use the renormalization time scale ε. In Fig. 2, the color represents the mean volatility $\langle \sigma^2 \rangle(\varepsilon, \Delta t)$ in dependence of ε and Δt, normalized by the average volatility $\bar{\sigma}$, where the brackets denote the average over all increasing microtrends (see Fig. 2a) or all decreasing microtrends (see Fig. 2b) in the full time series of $T_1 = 13{,}991{,}275$ records. If one can find $N_{\text{pos}}(\Delta t)$ positive microtrends and $N_{\text{neg}}(\Delta t)$ negative microtrends each of order Δt in the time series, and if $\sigma_i^2(\varepsilon)$ denotes the local volatility at position ε in the i-th positive or i-th negative microtrend, then the mean volatility is given by

$$\langle \sigma_{\text{pos}}^2 \rangle(\varepsilon, \Delta t) = \frac{1}{N_{\text{pos}}(\Delta t)} \sum_{i=1}^{N_{\text{pos}}(\Delta t)} \sigma_i^2(\varepsilon) \tag{6}$$

for positive microtrends and

$$\langle \sigma_{\text{neg}}^2 \rangle(\varepsilon, \Delta t) = \frac{1}{N_{\text{neg}}(\Delta t)} \sum_{i=1}^{N_{\text{neg}}(\Delta t)} \sigma_i^2(\varepsilon) \tag{7}$$

for negative microtrends. The mean volatility can be normalized by the average volatility $\bar{\sigma}$, which is determined by

$$\bar{\sigma}_{\text{pos}} = \frac{\varepsilon_{\text{bin}}}{\varepsilon_{\max} \Delta t_{\max}} \sum_{\varepsilon=0}^{\varepsilon_{\max}/\varepsilon_{\text{bin}}} \left(\sum_{\Delta t=0}^{\Delta t_{\max}} \langle \sigma_{\text{pos}}^2 \rangle(\varepsilon, \Delta t) \right) \tag{8}$$

and

$$\bar{\sigma}_{\text{neg}} = \frac{\varepsilon_{\text{bin}}}{\varepsilon_{\max} \Delta t_{\max}} \sum_{\varepsilon=0}^{\varepsilon_{\max}/\varepsilon_{\text{bin}}} \left(\sum_{\Delta t=0}^{\Delta t_{\max}} \langle \sigma_{\text{neg}}^2 \rangle(\varepsilon, \Delta t) \right), \tag{9}$$

where $\varepsilon_{\max}$ is the maximum value of the renormalization time scale ε studied, which is fixed to $\varepsilon_{\max} = 2$, and ε_{bin} denotes the bin size of the renormalization time scale. The maximum value of Δt analyzed is given by $\Delta t_{\max}$. For reasons of convenience, we relate the bin size to $\Delta t_{\max}$ via

$$\varepsilon_{\text{bin}} = \frac{\varepsilon_{\max}}{\Delta t_{\max}}. \tag{10}$$

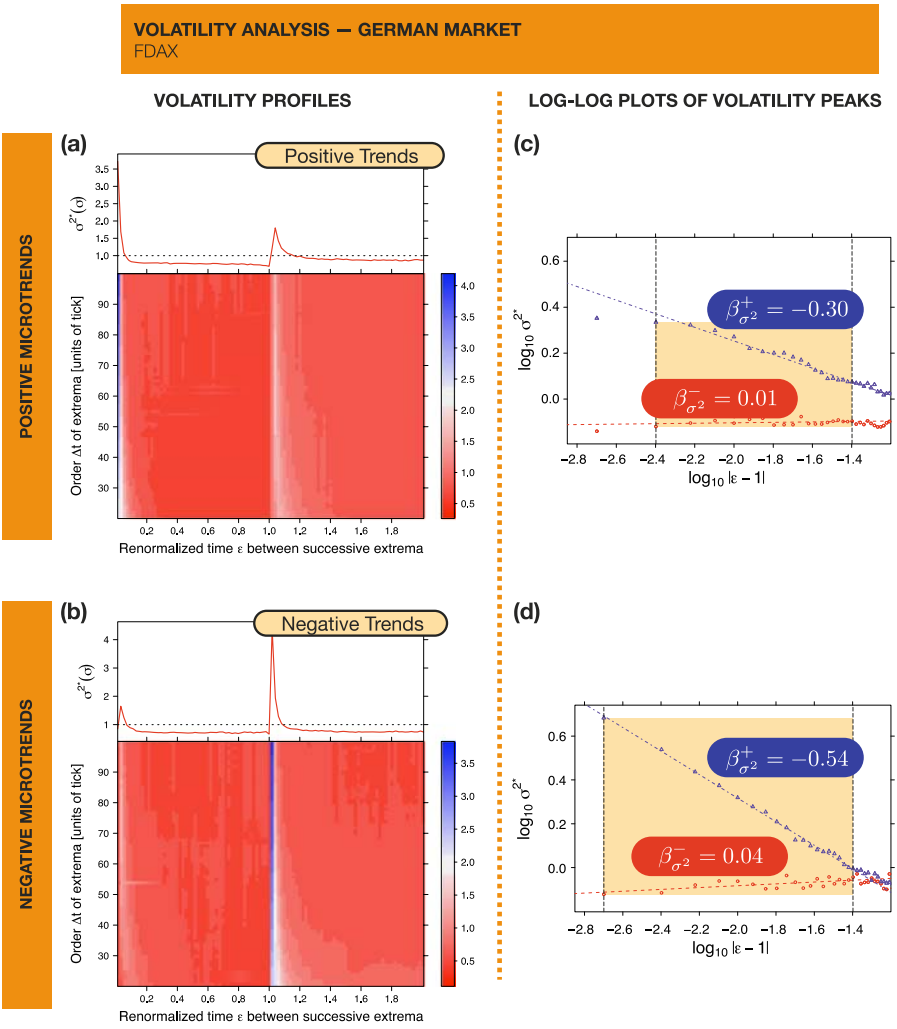

Fig. 2 Renormalization time analysis of volatility σ^2 for *microtrends*. (**a**) Volatility profile, averaged over all positive microtrends in the German DAX future time series and normalized by the average volatility of all positive microtrends studied. The color represents the normalized mean volatility $\langle\sigma^2_{\text{pos}}\rangle(\varepsilon, \Delta t)/\bar{\sigma}_{\text{pos}}$. The *color profile* shows the link between mean volatility and price evolution. New maximum values of the price time series are reached with a significant sudden jump of the volatility, as indicated by the *vertical white regions* and the sharp maximum in the volatility aggregation $\sigma^{2*}(\varepsilon)$ shown in the *top panel*. Here, $\sigma^{2*}(\varepsilon)$ denotes the average of the volatility profile, averaged only for layers with $50 \leq \Delta t \leq 100$. After reaching new maximum values in the price, the volatility decays and returns to the average value (*top panel*) for $\varepsilon > 1$. (**b**) Parallel analysis averaged over all negative microtrends in the time series. New minimum values of the price time series are reached with a pronounced sudden jump of the volatility, as indicated by the *vertical blue regions* in the volatility aggregation $\sigma^{2*}(\varepsilon)$ shown in the *top panel*. (**c**) Volatility (50 ticks $\leq \Delta t \leq$ 1000 ticks) before reaching a new maximum price value ($\varepsilon < 1$, *circles*) and after reaching a new maximum price value ($\varepsilon > 1$, *triangles*), aggregated for increasing microtrends. The *straight lines* correspond to power law scaling with exponents $\beta^+_{\sigma^2} = -0.30$ and $\beta^-_{\sigma^2} = 0.01$. The *shaded interval* marks the region in which this power law behavior is valid. (**d**) Log-log plot of $\sigma^{2*}(\varepsilon)$ for negative microtrends. The *straight lines* suggest power law scaling with exponents $\beta^+_{\sigma^2} = -0.54$ and $\beta^-_{\sigma^2} = 0.04$. The *left border of the shaded region* is given by the first measuring point closest to the switching point

The absence of changes of the colored volatility profiles in Fig. 2 is consistent with a *data collapse* for Δt values larger than a certain cut-off value Δt_{cut}. Thus, we calculate the volatility aggregation $\sigma^{2*}(\varepsilon)$. This volatility aggregation $\sigma^{2*}(\varepsilon)$ is the average of the mean volatility $\langle \sigma^2_{\mathrm{neg}} \rangle (\varepsilon, \Delta t)$, averaged only for layers with $\Delta t_{\mathrm{cut}} \leq \Delta t \leq \Delta t_{\mathrm{max}}$. It is given by

$$\sigma^{2*}_{\mathrm{pos}}(\varepsilon) = \frac{1}{\Delta t_{\mathrm{max}} - \Delta t_{\mathrm{cut}}} \sum_{\Delta t = \Delta t_{\mathrm{cut}}}^{\Delta t_{\mathrm{max}}} \frac{\langle \sigma^2_{\mathrm{pos}} \rangle (\varepsilon, \Delta t)}{\bar{\sigma}_{\mathrm{pos}}} \tag{11}$$

and the equivalent definition

$$\sigma^{2*}_{\mathrm{neg}}(\varepsilon) = \frac{1}{\Delta t_{\mathrm{max}} - \Delta t_{\mathrm{cut}}} \sum_{\Delta t = \Delta t_{\mathrm{cut}}}^{\Delta t_{\mathrm{max}}} \frac{\langle \sigma^2_{\mathrm{neg}} \rangle (\varepsilon, \Delta t)}{\bar{\sigma}_{\mathrm{neg}}} \tag{12}$$

for negative microtrends. Note that, in order to improve readability, we will drop the subscripts "pos" and "neg" in the following if the context determines whether positive or negative microtrends are considered.

The colored volatility profiles (see Fig. 2) show the mean volatility $\langle \sigma^2 \rangle (\varepsilon, \Delta t)$ averaged over all increasing or all decreasing microtrends in the full time series of $T_1 = 13{,}991{,}275$ records, and are normalized by the average volatilities of microtrends studied in both cases. In order to remove outliers, only such microtrends are collected in which the time intervals between successive trades $\tau(t)$ [39] are not longer than 1 minute, which is roughly 60 times longer than the average inter-trade time (≈ 0.94 s without overnight gaps), and in which the transaction volumes are not larger than 100 contracts (the average transaction volume is 2.55 contracts, see Table 1). This condition ensures that time t, when measured in units of ticks, runs only over the working hours of the exchange—removing overnight gaps, weekends, and national holidays.

The color profiles exhibit a link between volatility and price evolution. A new local price maximum is reached with a significant sudden jump of the volatility (top panel of Fig. 2a). After reaching new local maximum values in the price, the volatility decays and returns to the average value for $\varepsilon > 1$. Reaching a maximum seem to cause tension among the market participants. A local price maximum can stoke the expectations that higher prices are possible and thus stimulate purchases. However, this development can also raise fears of traders to find an optimal price for selling their assets. Additionally, it is possible that market participants hold a short position which means that they benefit from falling asset prices, having to stop their losses. For negative microtrends, the reaching of a local minimum value in the price coincides with a more pronounced sudden jump of the volatility (see Fig. 2b). A negative microtrend seems to create a situation in which market participants act in a more dramatic way after the end of a trend in comparison to the end of positive microtrends. One can conjecture that they are driven by tension at least or even by "panic", if they try to stop their losses. But of course, also the opposite situation should be relevant: A market participant who has no inventory is looking for entry opportunities. As asset prices are rising after reaching a local price minimum ($\varepsilon = 1$), a financial market actor who wants to enter into the market has to deal with the problem to find the "right" time—the optimal entry level, the local price minimum is already missed at this time.

This qualitative effect is intuitively understandable and should be obvious for market actors. In contrast, the shape of the volatility peak around extrema is surprising. The peak is characterized by asymmetric tails, as it is analyzed next. For this analysis, we use the volatility aggregation $\sigma^{2*}(\varepsilon)$, which is the mean volatility $\langle \sigma^2 \rangle (\varepsilon, \Delta t)$ averaged for layers from

$\Delta t_{\text{cut}} = 50$ ticks to $\Delta t_{\max} = 1000$ ticks. Figure 2c shows the aggregated average volatility $\sigma^{2*}(\varepsilon)$ for positive microtrends on a log-log plot. Surprisingly, the evolution of the volatility before and after reaching a maximum shows up as straight lines and thus are consistent with a power law scaling behavior

$$\sigma^{2*}(|\varepsilon - 1|) \sim |\varepsilon - 1|^{\beta_{\sigma^2}} \tag{13}$$

within the range indicated by the vertical dashed lines. Over one order of magnitude, we find distinct exponents, $\beta^{-}_{\sigma^2} = 0.01$ before a price maximum and $\beta^{+}_{\sigma^2} = -0.30$ after a price maximum. Figure 2d shows the aggregated average volatility $\sigma^{2*}(\varepsilon)$ for negative microtrends on a log-log plot. Over more than one order of magnitude, we find for negative microtrends a qualitatively consistent behavior with exponents $\beta^{-}_{\sigma^2} = 0.04$ before a price minimum and $\beta^{+}_{\sigma^2} = -0.54$ after it.

In the following, we will test the possible universality of our results by performing a parallel analysis for trends on long time scales, using the daily closing price data base of S&P500 stocks. Here, universality means that our renormalized market quantities do not change their values significantly for different markets, different time periods, or different market conditions.

Note that for our parallel analysis on macroscopic time scales, the order of a extremum Δt is measured in units of days, and that $\langle \sigma^2 \rangle(\varepsilon, \Delta t)$ is averaged additionally over the closing price time series of all S&P500 components. In order to avoid biased contributions for the rescaled averaging caused by inflation-based drifts over more than 47 years as described in section 2.2, the analyzed price time series $p(t)$ contains the logarithm of the daily closing prices. Figure 3a shows the mean volatility $\langle \sigma^2 \rangle(\varepsilon, \Delta t)$ for positive microtrends, averaged for layers from $\Delta t_{\text{cut}} = 10$ days to $\Delta t_{\max} = 100$ days. Figure 3b shows the mean volatility $\langle \sigma^2 \rangle(\varepsilon, \Delta t)$ for negative microtrends, averaged for the same layers' range. As already uncovered for microtrends, the sudden volatility rise is more dramatic for negative macrotrends than for positive macrotrends. Surprisingly, the aggregate average volatilities $\sigma^{2*}(\varepsilon)$ for positive and negative macrotrends on a log-log plot show again distinct tail exponents around the switching point $\varepsilon = 1$. For positive macrotrends, we obtain $\beta^{-}_{\sigma^2} = -0.05$ before a price maximum and $\beta^{+}_{\sigma^2} = -0.40$ after it. For negative microtrends, we obtain $\beta^{-}_{\sigma^2} = -0.09$ before a price minimum and $\beta^{+}_{\sigma^2} = -0.50$ after it, which is both similar to the values obtained for our study of positive and negative microtrends.

3.2 Volume Analysis

To test the possible universality of these results obtained for volatility, we perform a parallel analysis of the corresponding volume fluctuations $v(t)$, the numbers of contracts traded in each individual transaction in case of microtrends for the German market and the cumulative number of traded stocks per day in case of macrotrends for the US market. The volume profile provides the mean volume averaged over all increasing microtrends in the time series of the German market and is also normalized by the average volume of all microtrends studied. In order to remove outliers in this analysis, we consider only those microtrends which include inter-trade times not longer than 1 minute and transaction volumes not larger than 100 contracts. As expected, new price extrema are linked with peaks in the volume time series but, surprisingly, we find that the usual cross-correlation function between price changes and volumes vanishes. Thus, one can conjecture that the tendency towards increased volumes occurring at the end of positive microtrends is counteracted by the tendency towards

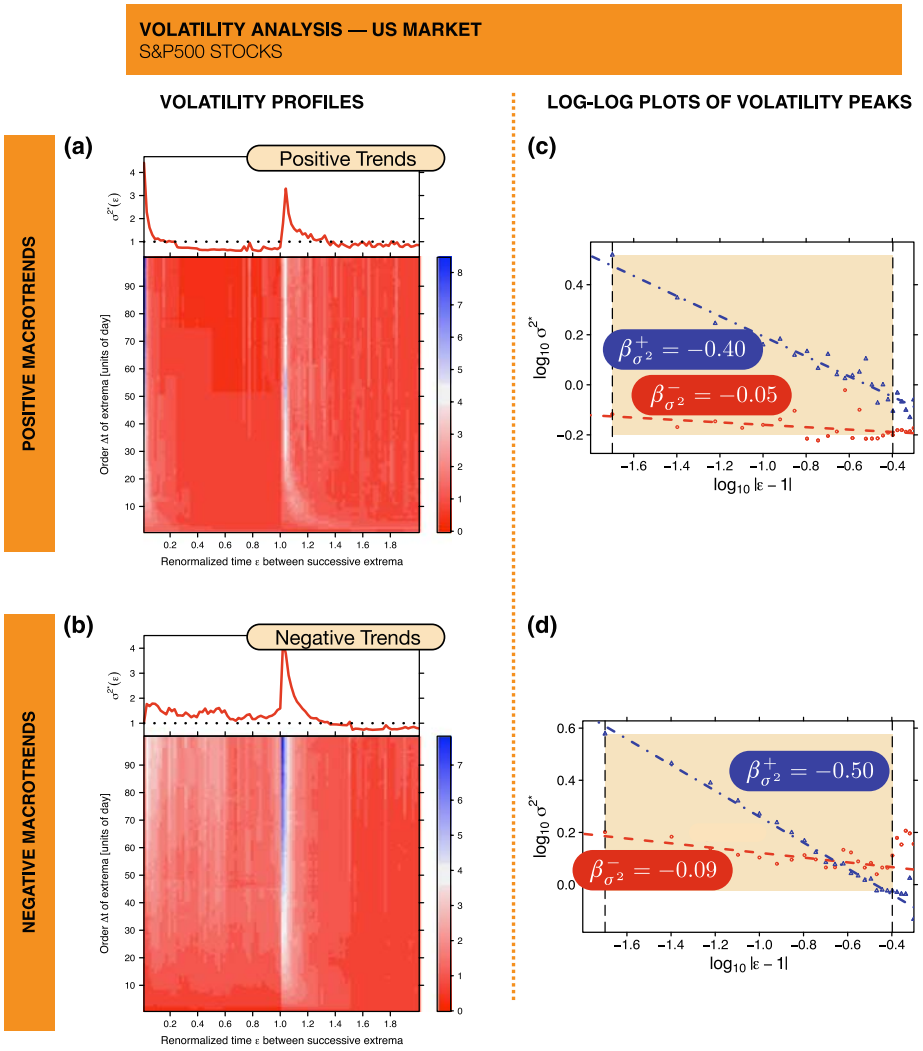

Fig. 3 Renormalization time analysis of volatility σ^2 for *macrotrends*. (**a**) Volatility profile, averaged over all positive macrotrends in the daily closing price time series of all S&P500 stocks and normalized by the average volatility of all positive macrotrends studied. The stylized fact that new maximum values of the price time series are reached with a significant sudden jump of the volatility can also be found for macrotrends. Note that Δt is measured in units of day for macrotrends. (**b**) Parallel analysis performed for all negative macrotrends in the daily closing price time series of all S&P500 stocks. As already uncovered for microtrends (see Fig. 2), the sudden jump of the volatility at $\varepsilon = 1$ is more pronounced for negative trends than for positive microtrends. (**c**) Volatility (10 days $\leq \Delta t \leq$ 100 days) before reaching a new maximum price value ($\varepsilon < 1$, *circles*) and after reaching a new maximum price value ($\varepsilon > 1$, *triangles*), aggregated for increasing macrotrends. The *straight lines* suggest power law scaling with exponents $\beta^+_{\sigma^2} = -0.40$ and $\beta^-_{\sigma^2} = -0.05$. (**d**) Log-log plot of $\sigma^{2*}(\varepsilon)$ for negative macrotrends. The *straight lines* correspond to power law scaling with exponents $\beta^+_{\sigma^2} = -0.50$ and $\beta^-_{\sigma^2} = -0.09$

increased volumes occurring at the end of negative microtrends. The crucial issue is to distinguish between positive and negative microtrends, realized by the renormalization time ε between successive extrema.

For positive microtrends, a significant increase of volumes can be found already before the local maximum price is reached. After reaching the local maximum value, the volatility falls dramatically back to values close to the average value. For negative microtrends, the opposite characteristic is observed. Reaching a local price minimum causes a sudden jump of the transaction volume, whereas after the local price minimum the volume decays and returns to the average value for $\varepsilon > 1$. We find

$$v^*(|\varepsilon - 1|) \sim |\varepsilon - 1|^{\beta_v} \tag{14}$$

with exponents $\beta_v^- = -0.14$ before and $\beta_v^+ = -0.20$ after a price maximum. $v^*(\varepsilon)$ is obtained by averaging Δt "slices" between $\Delta t_{\text{cut}} = 50$ and $\Delta t_{\max} = 1000$. For negative microtrends, straight lines can be fitted to the log-log histogram as well with exponents $\beta_v^- = -0.17$ before and $\beta_v^+ = 0$ after a local price minimum.

A parallel analysis for the US market on large time scales provides evidence that the volume peaks are symmetrically shaped around the switching point $\varepsilon = 1$ and that the characteristics are similar for positive and negative macrotrends. The power law exponents for positive microtrends are given by $\beta_v^- = -0.04$ before, and $\beta_v^+ = -0.08$ after a local price maximum. The similar behavior of negative microtrends is supported by exponents $\beta_v^- = -0.05$ before and $\beta_v^+ = -0.15$ after a local price minimum.

3.3 Inter Trade Time Analysis

In order to verify a possible universality, we analyze additionally the behavior of the inter-trade times $\tau(t)$ of the German market during the short time interval from one price extremum to the next. The linear cross-correlation function between price changes and inter-trade times as standard tool of time series analysis exhibits no significant correlation values as well. Thus, one can again conjecture that the tendency towards decreased inter-trade times at the end of positive microtrends is counteracted by the tendency towards decreased inter-trade times at the end of negative microtrends. It is of crucial importance to distinguish between positive and negative microtrends. The mean inter-trade time $\langle\tau\rangle(\varepsilon, \Delta t)/\bar{\tau}$ reflects a link between inter-trade times and price extrema. Far away from the critical point $\varepsilon = 1$, the mean inter-trade time starts to decrease. After the formation of a new local price maximum, the mean inter-trade times increase and return to the average value in a symmetrical way. Negative microtrends obey the same behavior with one exception. Reaching a local price minimum ($\varepsilon = 1$) coincides with a temporary sudden increase of the inter-trade times. For both types of trends, the dip of the inter-trade times may be interpreted in terms of "panic". Already before reaching local extremal prices, market actors try to participate in the forming trend or try to correct their trading decision, which was caused by the hope to participate in the establishment of an opposite trend. After reaching the local extremal price, the tension persists, but becomes steadily smaller. We find

$$\tau^*(|\varepsilon - 1|) \sim |\varepsilon - 1|^{\beta_\tau} \tag{15}$$

for positive microtrends with exponents $\beta_\tau^- = 0.10$ before and $\beta_\tau^+ = 0.12$ after a local price maximum. For negative microtrends, we obtain exponents $\beta_\tau^- = 0.09$ before and $\beta_\tau^+ = 0.15$ after a local price minimum. A log-log histogram of a parallel analysis for the US market on large time scales is not obtainable, as the inter-trade times between successive closing prices are given by the constant value of 1 day (exceptions are weekends and general holidays).

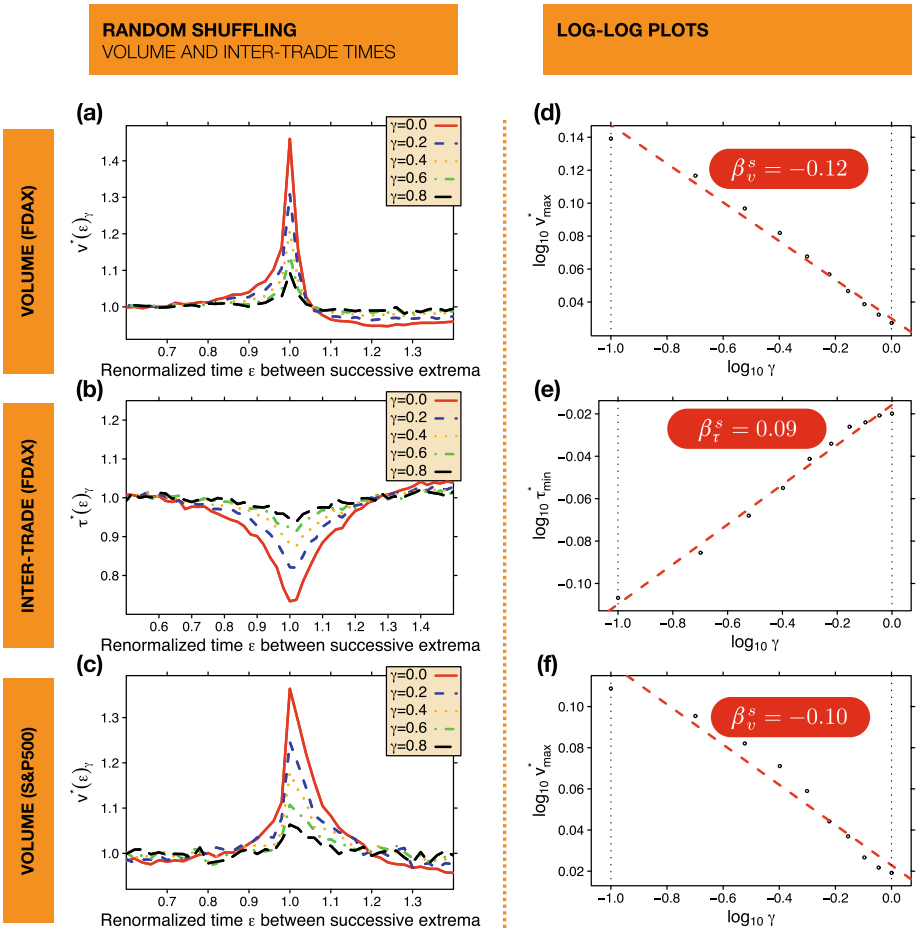

Fig. 4 Stability test of the power law dependence. (**a**) If one reshuffles randomly γT pairs of volume entries in the multivariate time series, the significant link between volume and price evolution starts to disappear as γ increases. (**b**) If γT pairs of inter-trade time entries are randomly reshuffled, the inter-trade time dip starts to disappear. (**c**) We find an identical behavior for the volume peak on long time scales, using daily closing prices of S&P500 stocks. (**d**) The disappearance phenomenon appears to follow a power law behavior. The maximum value of $v^*(\varepsilon)_\gamma$ at $\varepsilon = 1$ scales with exponent $\beta_v^s = -0.115 \pm 0.005$. (**e**) The minimum value of $\tau^*(\varepsilon)_\gamma$ at $\varepsilon = 1$ scales with exponent $\beta_v^s = 0.094 \pm 0.004$. (**f**) In the case of the maximum of $v^*(\varepsilon)_\gamma$ at $\varepsilon = 1$ for the S&P500 stocks, the plot may be fitted by a power law with exponent $\beta_v^s = -0.095 \pm 0.008$

3.4 Random Reshuffling

To confirm that our results are a consequence of the exact time series sequence and thus sensitive to the time ordering of the original time series of volumes and inter-trade times, we randomly reshuffle (γT) pairs of data points of both the volume time series and inter-trade time series in order to weaken their connection with the price evolution. We find that the clear link between volumes fluctuations and price evolution (see Fig. 4a) and between inter-trade times and price evolution (see Fig. 4b) disappears with increasing γ and entirely vanishes for $\gamma \geq 1$ for microtrends. The dip of the inter-trade times at $\varepsilon = 1$ becomes less pronounced with increasing γ and, correspondingly, the peak of the volume maximum de-

creases. For the S&P500 data set (Fig. 4c), the volume peak disappears with increasing γ, obeying the same characteristics. These reshuffling induced processes may be characterized by power law relationships as well, which support our finding that a fluctuating price time series passes through a sequence of distinct transitions with scale-free properties. The disappearance phenomenon follows a power law behavior. The maximum value of $v^*(\varepsilon)_\gamma$ at $\varepsilon = 1$ scales with exponent $\beta_v^s = -0.12$ for microtrends (Fig. 4d). The minimum value of $\tau^*(\varepsilon)_\gamma$ at $\varepsilon = 1$ scales with exponent $\beta_v^s = 0.09$ as shown in Fig. 4e. In the case of the maximum of $v^*(\varepsilon)_\gamma$ at $\varepsilon = 1$ on large time scales, the log-log plot can be fitted by a straight line with a power law exponent $\beta_v^s = -0.10$ for the S&P500 stocks. However, some deviations can be observed for macrotrends, which are caused by the limited number of closing prices in the S&P500 data set ($T_2 \ll T_1$).

Using this approach, it is not possible to reshuffle the volatility as it is extracted directly from the price time series. As our study pursues a data-driven approach and finds a higher volatility around the switching point, we have to clarify, whether the increase in variance is caused by the application of the variance formula to a time series with a changing trend. The relevance of the trend dynamics for the variance can, for example, be seen in [40]. In general, the tendency towards higher volatility around switching points can be qualitatively obtained by a random walk process. However, this does not effect the results of volume and inter-trade times [41].

4 Summary and Conclusions

The straight lines in Fig. 5 offer insight into financial market fluctuations: (i) a clear connection between volatility, volumes, inter-trade times, and price fluctuations on the path from one extremum to the next extremum, and (ii) the underlying law, which describes the tails of volatility, volumes, and inter-trade times around extrema varying over 9 orders of magnitude starting from the smallest possible time scale, is a power law with a unique exponents which quantitatively characterize the region around the trend switching point. As a direct consequence of the existence of power law tails, the behavior does not depend on the scale. Thus, we find identical behavior for other sub-intervals of $50 \leq \Delta t \leq 1000$. With a decreasing value of Δt, the number of local minima and maxima increases (see Fig. 1), around which we find scale-free behavior, for exactly the same ε interval $0.6 \leq \varepsilon \leq 1.4$. The peaks in $\sigma^2(\varepsilon)$ and $v(\varepsilon)$ around $\varepsilon = 1$ and the dip of $\tau(\varepsilon)$ around $\varepsilon = 1$ offer a challenge for multi-agent-based financial market models [42–48] to reproduce these empirical facts. The characterization of volatility, volume, and inter-trade times by power law relationships in the time domain supports our hypothesis that a fluctuating price time series passes through a sequence of "phase transitions".

Before concluding, we may ask "what kind of phase transition" could the end of a microtrend or macrotrend correspond to, or is the end of a trend an altogether different kind of phase transition that resembles all phase transitions by displaying a regime of scale free behavior characterized by a critical exponent? It may be premature to speculate on possible analogies, so we will limit ourselves to describing here what seems to be a promising candidate. Consider a simple Ising magnet characterized by one-dimensional spins that can point North or South. Each spin interacts with some (or even with all) of its neighbors with positive interaction strength J, such that, when J is positive neighboring spins lower their energy by being parallel. The entire system is bathed in a magnetic field that interacts with all the spins equally with a strength parametrized by H, such that when H is positive, the field points North and when H is negative the field points South. Thus, when H is positive,

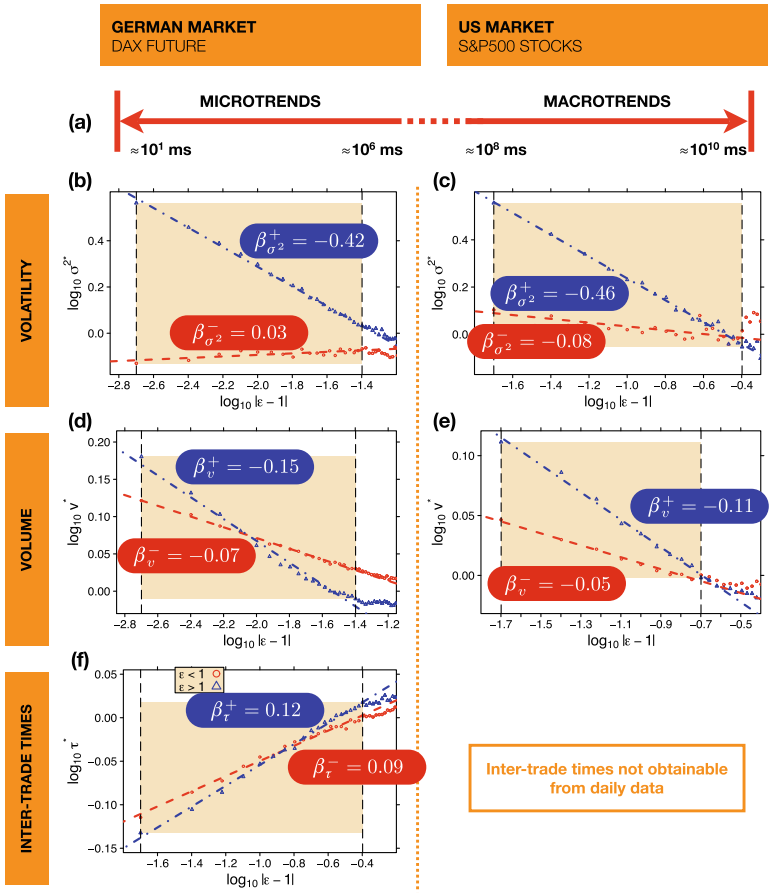

Fig. 5 Overview of time scales studied and log-log plots of quantities with scale-free properties. (**a**) Visualization of time scales studied for both the German market and the US market. For the analysis of microtrends, we use the German DAX future data base which enables us to analyze microtrends starting at roughly 10^6 ms down to the smallest possible time scale of individual transactions measured in multiples of 10 ms. The log-log plots of quantities with scale-free behavior on short time scales are shown in the *left column*. For the analysis of macrotrends, we use the data base of daily closing prices of all S&P500 stocks, which enables us to perform equivalent analysis of macrotrends on long time scales which are shown the *right column*. Thus, our analysis of switching processes ranges over 9 orders of magnitude from 10 ms to 10^{10} ms. (**b**) Volatility (50 ticks $\leq \Delta t \leq$ 1000 ticks) before reaching a new extreme price value ($\varepsilon < 1$, *circles*) and after reaching a new extreme price value ($\varepsilon > 1$, *triangles*), aggregated for microtrends. The *straight lines* suggest power law scaling with exponents $\beta^+_{\sigma^2} = -0.42 \pm 0.01$ and $\beta^-_{\sigma^2} = 0.03 \pm 0.01$. The *shaded interval* marks the region in which this power law behavior is valid. The *left border of the shaded region* is given by the first measuring point closest to the switching point. (**c**) Volatility aggregation of macrotrends determined for the US market on long time scales (10 days $\leq \Delta t \leq$ 100 days). The *straight lines* correspond to power law scaling with exponents $\beta^+_{\sigma^2} = -0.46 \pm 0.01$ and $\beta^-_{\sigma^2} = -0.08 \pm 0.02$, which seem to be similar to the exponents determined for the German future market on short time scales. (**d**) Log-log plot of the volume aggregation on short time scales (50 ticks $\leq \Delta t \leq$ 1000 ticks) exhibiting a power law behavior with exponents $\beta^+_v = -0.146 \pm 0.005$ and $\beta^-_v = -0.072 \pm 0.001$. (**e**) Log-log plot of the volume aggregation on long time scales (10 days $\leq \Delta t \leq$ 100 days) exhibits a power law behavior with exponents $\beta^+_v = -0.115 \pm 0.003$ and $\beta^-_v = -0.050 \pm 0.002$, seem to be similar to our results on short time scales. (**f**) Log-log plot of the inter-trade time aggregation on short time scales (50 ticks $\leq \Delta t \leq$ 100 ticks), exhibiting a power law behavior with exponents $\beta^+_\tau = 0.120 \pm 0.002$ and $\beta^-_\tau = 0.087 \pm 0.002$. An equivalent analysis of long time scales is not possible, as daily closing prices are recorded with equidistant time steps

the system lowers its energy by each spin pointing North. Thus, there are two competing control parameters J and H. If, e.g., the system is prepared in a state with the majority of spins pointing North yet the field H points South, the competition will be between the relative effects of J and H: the J interaction motivates the spins to point North but the H interaction motivates the spin to point South. Such a system is termed *metastable* since, if each North-pointing spin suddenly flips its state to point South, the system can achieve a lower total energy. This flipping will occur in time in a fashion not unlike the trading frequency near the end of a trend: first, one or two spins will randomly switch their state, then more, and suddenly, after in an "avalanche" of switches, the majority of spins will point South. The phase transition is termed a spinodal singularity, characterized by its own set of exponents.

Why should the end of microtrends or macrotrends have a parallel with such a metastable physical system? Presumably, near the end of a positive trend, all the market participants watching the market begin to sense that the market is metastable and that, if they do not sell soon, it could be too late to make any profit, because the price will drop. First, a few traders sell, pushing the market imperceptibly lower. Then, additional traders, sensing this microscopic downturn, may decide that now is the time to sell and they sell too. Then an "avalanche" of selling begins, with traders all hoping to protect their profits by selling before the market drops. Thus, the set of N market participants "holding their position" are in this sense analogous to the set of N mostly North-pointing spins, bathed in a South-pointing magnetic field.

Perhaps, the above analogy is not yet the best. It will be a future challenge to find a coherent, convincing explanation for why the end of a microtrend or macrotrend displays such striking parallels to a phase transition. In any case, a set of interacting spins appears to be analogous to a set of interacting traders.

The end of the negative microtrend or macrotrend follows the same mechanism, but with everything reversed. The N Ising spins point mostly South, the magnetic field points North, and the spins flip from South to North one by one, ending with an avalanche corresponding to the spinodal singularity. Analogously, the N traders begin to suspect that the market is becoming metastable, so that they start to buy one by one. But as the traders witness the price increasing, they jump into buy mode before the price becomes too high.

In summary, we have seen that each trend—microtrend and macrotrend—in a financial market starts and ends with a unique switching process, and each extremum shares properties of macroscopic cooperative behavior. We have seen that the mechanism of bubble formation and bubble bursting has no scale, for time scales varying over 9 orders of magnitude down to the smallest possible time scale—the scale of single transactions measured in units of 10 ms. On large time scales, histograms of price returns provide the same scale-free behavior. Thus, the formation of positive and negative trends on all scales is a fundamental principle of trading, starting on the smallest possible time scale, which leads to the non-stationary nature of financial markets as well as to crash events on large time scales. Thus, the well-known catastrophic bubbles occurring on large time scales—such as the most recent financial crisis—may not be outliers but in fact single dramatic events caused by the inherent, scale-free behavior related to the formation of increasing and decreasing trends on time scales from the very large down to the very small.

Acknowledgements The authors thank K. Binder, S.V. Buldyrev, C. De Grandi, S. Havlin, D. Helbing, U. Krey, H.-G. Matuttis, M.G. Mazza, I. Morgenstern, W. Paul, J.J. Schneider, R.H.R. Stanley, T. Vicsek, and G.M. Viswanathan for discussions, and we also thank the German Research Foundation (DFG), the Gutenberg Academy, and the NSF for financial support.

References

1. Anderson, P.W.: Science **177**, 393 (1972)
2. Stanley, H.E.: Rev. Mod. Phys. **71**, S358 (1999)
3. Mantegna, R.N., Stanley, H.E.: Introduction to Econophysics Correlations and Complexity in Finance. Cambridge Univ. Press, Cambridge (2000)
4. Axtell, R.L.: Science **293**, 1818 (2001)
5. Takayasu, H. (ed.): Practical Fruits of Econophysics. Springer, Berlin (2006)
6. Kiyono, K., Struzik, Z.R., Yamamoto, Y.: Phys. Rev. Lett. **96**, 068701 (2006)
7. Watanabe, K., Takayasu, H., Takayasu, M.: Physica A **383**, 120 (2007)
8. Gabaix, X., Gopikrishnan, P., Plerou, V., Stanley, H.E.: Nature **423**, 267 (2003)
9. Preis, T., Paul, W., Schneider, J.J.: Europhys. Lett. **82**, 68005 (2008)
10. Preis, T., Virnau, P., Paul, W., Schneider, J.J.: New J. Phys. **11**, 093024 (2009)
11. Lillo, F., Farmer, J.D., Mantegna, R.N.: Nature **421**, 129 (2003)
12. Plerou, V., Gopikrishnan, P., Gabaix, X., Stanley, H.E.: Phys. Rev. E **66**, 027104 (2002)
13. Cont, R., Bouchaud, J.P.: Macroecon. Dyn. **4**, 170 (2000)
14. Krawiecki, A., Holyst, J.A., Helbing, D.: Phys. Rev. Lett. **89**, 158701 (2002)
15. O'Hara, M.: Market Microstructure Theory. Blackwell, Cambridge (1995)
16. Vandewalle, N., Ausloos, M.: Physica A **246**, 454 (1997)
17. Eisler, Z., Kertész, J.: Phys. Rev. E **73**, 046109 (2006)
18. Mandelbrot, B.: J. Bus. **36**, 394 (1963)
19. Fama, E.F.: J. Bus. **36**, 420 (1963)
20. Lux, T.: Appl. Financ. Econ. **6**, 463 (1996)
21. Guillaume, D.M., Dacorogna, M.M., Davé, R.R., Müller, U.A., Olsen, R.B., Pictet, O.V.: Financ. Stoch. **1**, 95 (1997)
22. Gopikrishnan, P., Meyer, M., Amaral, L., Stanley, H.E.: Eur. J. Phys. B **3**, 139 (1998)
23. Plerou, V., Gopikrishnan, P., Rosenow, B., Amaral, L.A.N., Stanley, H.E.: Phys. Rev. Lett. **83**, 1471 (1999)
24. Gopikrishnan, P., Plerou, V., Amaral, L.A.N., Meyer, M., Stanley, H.E.: Phys. Rev. E **60**, 5305 (1999)
25. Gopikrishnan, P., Plerou, V., Gabaix, X., Stanley, H.E.: Phys. Rev. E **62**, 4493 (2000)
26. Krugman, P.: The Self-Organizing Economy. Blackwell, Cambridge (1996)
27. Shleifer, A.: Inefficient Markets: An Introduction to Behavioral Finance. Oxford Univ. Press, Oxford (2000)
28. Helbing, D., Farkas, I., Vicsek, T.: Nature **407**, 487 (2000)
29. Bunde, A., Schellnhuber, H.J., Kropp, J. (eds.): The Science of Disasters: Climate Disruptions, Heart Attacks, and Market Crashes. Springer, Berlin (2002)
30. Jones, C.M., Kaul, G., Lipson, M.L.: Rev. Financ. Stud. **7**, 631 (1994)
31. Chan, L., Fong, W.M.: J. Financ. Econ. **57**, 247 (2000)
32. Politi, M., Scalas, E.: Physica A **387**, 2025 (2008)
33. Jiang, Z.Q., Chen, W., Zhou, W.X.: Physica A **388**, 433 (2009)
34. Dubil, R.: An Arbitrage Guide to Financial Markets. Wiley, Chichester (2004)
35. Deutsch, H.P.: Derivate und Interne Modelle: Modernes Risk Management. Schaefer-Poeschel, Stuttgart (2001)
36. Binder, K.: Rep. Prog. Phys. **50**, 783 (1987)
37. Peng, C.K., Mietus, J., Hausdorff, J.M., Havlin, S., Stanley, H.E., Goldberger, A.L.: Phys. Rev. Lett. **70**, 1343 (1993)
38. Helbing, D., Huberman, B.A.: Nature **396**, 738 (1998)
39. Ivanov, P.C., Yuen, A., Podobnik, B., Lee, Y.: Phys. Rev. E **69**, 056107 (2004)
40. Helbing, D.: Phys. Rev. E **55**, R25 (1996)
41. Preis, T., Schneider, J.J., Stanley, H.E.: Formation and bursting of financial bubbles. Preprint (2009)
42. Smith, E., Farmer, J.D., Gillemot, L., Krishnamurthy, S.: Quant. Finance **3**, 481 (2003)
43. Lux, T., Marchesi, M.: Nature **397**, 498 (1999)
44. Preis, T., Golke, S., Paul, W., Schneider, J.J.: Europhys. Lett. **75**, 510 (2006)
45. Preis, T., Golke, S., Paul, W., Schneider, J.J.: Phys. Rev. E **76**, 016108 (2007)
46. Bouchaud, J.P., Matacz, A., Potters, M.: Phys. Rev. Lett. **87**, 228701 (2001)
47. Haerdle, W., Kleinow, T., Korostelev, A., Logeay, C., Platen, E.: Quant. Financ. **8**, 81 (2008)
48. Halla, A.D., Hautsch, N.: J. Financ. Mark. **10**, 249 (2007)